

Laser Thomson Scattering Diagnostics of Dielectric Barrier Discharge Plasmas

Yasushi SONODA, Shuhei NISHIMOTO, Kentaro TOMITA, Safwat HASSABALLA,
Yukihiko YAMAGATA, Kiichiro UCHINO

Interdisciplinary Graduate School of Engineering Sciences, Kyushu University, Kasuga, Fukuoka, 816-8580, Japan

(Received: 12 September 2008 / Accepted: 6 December 2008)

Applications of Thomson scattering diagnostics to two kinds of dielectric barrier discharge (DBD) plasmas are presented. One is that for the plasma display panel. In order to avoid laser perturbations for Xe containing discharges which are easily disturbed by laser beams with visible wavelengths, a laser Thomson scattering (LTS) system having an infrared laser (wavelength 1064 nm) as a light source has been developed. The other is the capacity coupled discharge (CCD) which was produced between needle and sphere electrodes. Electron densities and electron temperatures of CCD plasmas were evaluated quantitatively for the first time.

Keywords: laser thomson scattering, dielectric barrier discharges, capacity coupled discharge, plasma display panel, laser perturbation, electron density, electron temperature

1. Introduction

Dielectric Barrier Discharges (DBD) are created in a high pressure gas at around 1 atm, and produce non-thermal plasmas. The DBD plasmas are used for many applications such as the production of ozone, a plasma display panel, and the treatment of harmful exhausted gases. However, detailed plasma parameters of the DBD plasmas have not yet been known.

In order to assist understanding of DBD plasmas, we have been developing the laser Thomson scattering (LTS) as a diagnostic method of DBD plasmas. We picked up two kinds of DBD plasmas. One was that for the plasma display panel (PDP) which was produced on a coplanar electrode system covered by a dielectric material. The other was the capacity coupled discharge (CCD) which was produced between a needle and a spherical electrode.

2. Diagnostics of PDP plasmas

2.1 Summary of LTS measurements using a visible system

For our first LTS system, we used the second harmonics beam of the Nd:YAG (wavelength 532 nm) laser as a light source. When we applied the LTS method to micro-discharge plasmas, there were two main difficulties, namely the small scattering volume and the high stray light level. The small size of micro-discharge plasmas implies a small scattering volume, which results in a very small Thomson scattering signal. This difficulty could be overcome by using the photon counting accompanied by data accumulation method.

The second difficulty is that the stray laser light is

very strong because the wall of the discharge cell is very close to the discharge volume. In order to overcome this problem, we designed a special triple grating spectrometer (TGS). The stray light rejection factor of the TGS was measured to be 10^{-8} at $\Delta\lambda = 1$ nm away from the laser wavelength. This high rejection allowed us to apply the LTS method to micro-discharge plasmas [1].

By using this system the striation phenomenon which had been universally observed above the anode of ac-PDP [2], was investigated. The discharge was produced in the Ne/Ar (10%) gas mixture at a pressure of 200 Torr. Results of the LTS measurements showed modulations in both n_e and T_e profiles above the anode, and these modulations had a similar trend to striations appeared in the optical emission images. Also, it was found that the modulations in n_e and T_e were out of phase [3].

When we injected the second harmonics beam of the Nd:YAG laser into discharges in gas mixtures containing the Xe gas, we observed abnormally large signals. The large signals were also observed even when there was no discharge plasma. In order to investigate this phenomenon, we injected the second harmonics beam of the Nd:YAG laser at different energies into a pure Ne gas at 200 Torr and a gas mixture of Ne/Xe (10%) at 200 Torr. For the pure Ne gas, no signal was observed. On the other hand, for the gas mixture of Ne/Xe, signals appeared and increased steeply above the laser energy E_L of 5 mJ. This implies that Xe atoms at the ground state (ionization potential 12.1 eV) were ionized by the laser with $E_L > 5$ mJ. In fact, the steep increase of the signal in the range $5 \text{ mJ} < E_L < 8 \text{ mJ}$ was consistent with 7-photon absorption process (6 photons for multi-photon ionization and 1 photon for Thomson

e-mail: uchino@ence.kyushu-u.ac.jp

scattering). The lower photon energy of the laser will be favorable to avoid the laser perturbation of the discharge.

2.2 Infrared LTS system

The configuration of the electrodes used in this study is shown in Fig. 1. The structure was similar to the sustaining electrodes of a coplanar ac-PDP. The electrodes were built on a glass substrate which has a width of 2 mm and a thickness of 3 mm. The electrodes had a discharge gap of 0.1mm. The electrodes were covered with a 15 μm glass layer, followed by a 0.5 μm MgO layer.

Figure 2 shows the schematic diagram of the experimental setup. The system was similar to the system using a visible light source. Differences were the laser light source having a wavelength of 1064 nm and the optical components, such as achromatic lenses and gratings used in the TGS, which were designed for 1064 nm. Also, the detector was for 1064 nm, namely an infrared photomultiplier tube (Hamamatsu, R5509) which had a quantum efficiency of $\sim 5\%$ at 1064 nm and could be used for the photon counting.

The electrode substrate was housed in the chamber. After evacuating the discharge chamber, the Ne/Xe gas mixture was introduced. Alternating voltage pulses with a square waveform were applied between the electrodes at a frequency of 20 kHz and duty ratio of 0.4. The peak value of the applied pulse voltage was 270 V.

Figure 3 shows the schematic diagram of the homemade TGS for the infrared system. The observation wavelength of the system was tuned by rotating the three gratings of the infrared TGS, and we confirmed that

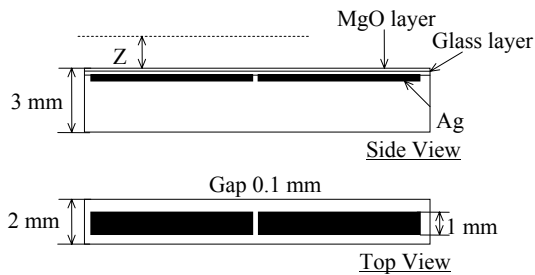


Fig.1 Schematic diagram of the geometrical structure of the electrodes.

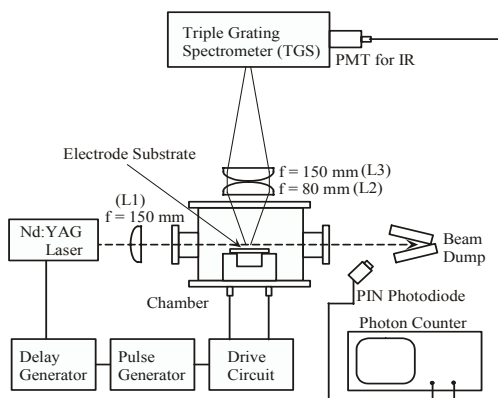


Fig.2 Experimental setup.

rotation angles of these gratings were just as calculated, optical components of the TGS were properly arranged at designed positions. The most important design parameters were the grating constant 900 grooves/mm, focal lengths of lenses, and differential angles of incidence and reflection of gratings to be 30°. Focal lengths of lenses placed between the slit 1 and the slit 4 were all 200 mm. Three gratings were arranged so that dispersions of three gratings were additive. An inverse dispersion at a surface of the slit 4 was 5.2 nm/mm.

Measured spectral profiles of the stray light using the TGS for the infrared system are shown in Fig. 4. In order to obtain these profiles, we first adjusted gratings 1 and 2 in Fig. 3 so that lights at the central laser wavelength (1064 nm) pass through slits 2 and 3. Then the grating 3 was tuned to cover the spectral range of ± 6 nm away from the laser wavelength. This way, we obtained the profile shown by triangle data points. This is the usual stray light profile of a single grating spectrometer and indicates that the stray light rejection at $\Delta\lambda = 2$ nm away from the laser wavelength is in the range from 10^{-3} to 10^{-4} . Next, we

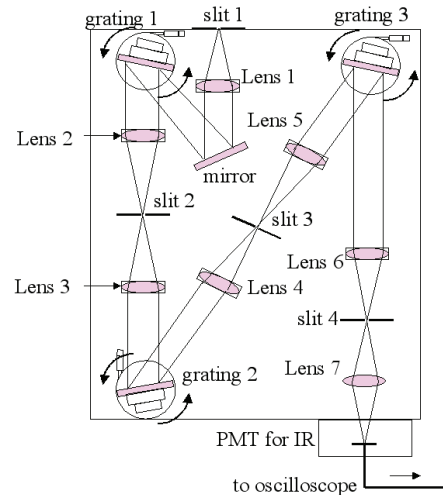


Fig.3 Schematic diagram of the triple grating spectrometer for the infrared laser system.

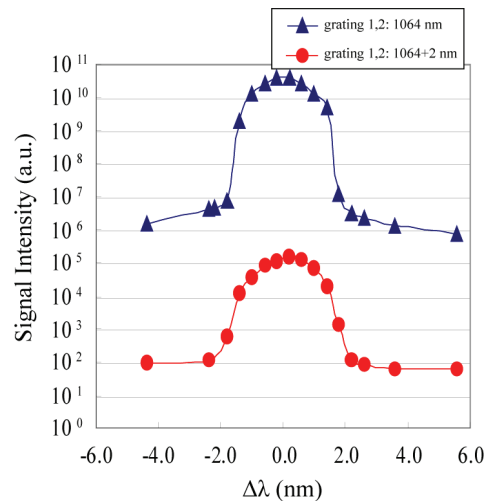


Fig.4 Measured spectral profiles of the stray light by the infrared laser system.

adjusted gratings 1 and 2 so that lights at a wavelength of 1066 nm pass through slits 2 and 3. Again, the grating 3 was tuned as before. The profile shown by circle data points is obtained this way. In this profile, an actually meaningful point is that at $\Delta\lambda = 2$ nm for which all gratings were tuned to the wavelength of 1066 nm. The stray light intensity at this point is below 10^{-8} compared to the point for which all gratings were tuned to the laser wavelength (the center point of the profile shown by triangle data points). This means that the performance of the TGS for the infrared system is comparable to that of the TGS for the visible system.

The performance of the LTS system was examined by conducting Raman scattering measurements from hydrogen gas. One of the rotational Raman scattering lines of the hydrogen gas was observed at about 41 nm away from the laser wavelength on the longer wavelength side. The absolute intensity of the observed Raman signal was 80 counts per 1000 laser shots when the laser energy was 20 mJ and hydrogen gas pressure was 100 Torr. This Raman signal corresponds to the Thomson scattering signal from the plasma having an electron density of $2 \times 10^{18} \text{ m}^{-3}$. For the actual measurements, the Thomson scattering spectra should be analyzed by observing the scattering intensity at several differential wavelengths. Nevertheless, we can expect enough signal-to-noise ratios for Thomson signals when the electron density is more than $1 \times 10^{19} \text{ m}^{-3}$. After confirming the performance of the infrared LTS system to be sufficient, we performed measurements of n_e and T_e distributions in plasmas produced in Ne/Xe gas mixtures.

2.3 Results and discussion

2.3.1 Laser Perturbations

Detailed experimental measurements have been performed to investigate the influence of the fundamental output of the Nd:YAG laser on Ne/Xe gas mixtures and Ne/Xe plasmas. In case of Ne/Xe gas mixtures we could not observe any signals, indicating that there is no photo ionization from ground state Xe atoms. On the other hand, for Ne/Xe plasma the linearity of LTS signals against the laser energy was investigated as shown in Fig. 5 for (a) Ne/Xe (10%) and (b) Ne/Xe (20%). In Fig. 5, the solid lines show that the signal is linearly proportional to the laser energy and dotted lines show that the signal is proportional to the 4th power of laser energy. Here, the laser energy of 4 mJ corresponds to the laser intensity of 10^{15} W/m^2 . These measurements were carried out at the points where largest LTS signals were observed. Other conditions were fixed as follows. Gas pressure was 200 Torr, observation time was 270 ns from the start of the discharge, and the observed wavelength was at $\Delta\lambda = 2.6$ nm from the laser wavelength.

It can be seen from Fig. 5(a) that the LTS signal is linearly proportional to laser energy in the range < 20 mJ.

While for laser energy > 20 mJ, the LTS signals deviate from the linearity and proportional to the 4th power of laser energy. This 4th power dependence can be due to the photo-ionization of meta-stable Xe atoms by 3 photon absorption. For higher Xe percentages, as shown in Fig. 5(b), LTS signals deviate from the linearity at lower laser energy. This can be due to the increase of the excited Xe density with the increase of Xe percentage.

Obviously, LTS measurements must be done with the laser energy in the linear ranges of Fig. 5. Therefore, for new discharge conditions signal linearity against laser energy must be checked before the full measurements of scattered spectra.

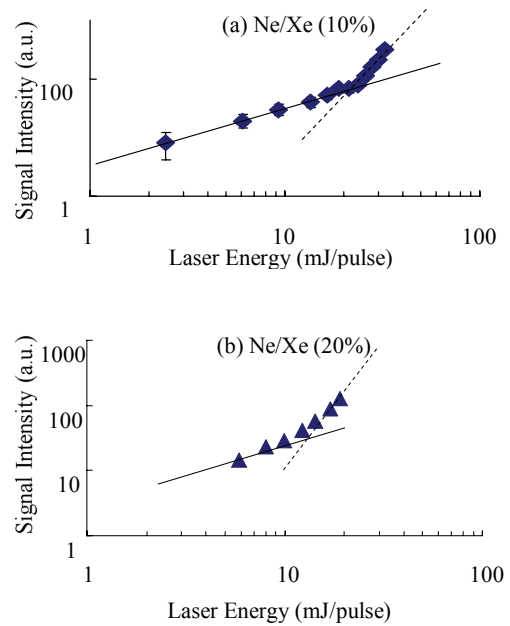


Fig. 5 LTS signal intensity against laser energy.

2.3.2 Results of LTS measurements

Figure 6 shows distributions of the LTS signals along the electrode surface for different Xe percentages of 5, 10, and 30%. Measurements were performed at a fixed height of 100 μm above the electrode surface and at a fixed wavelength ($\Delta\lambda = 2.6$ nm). The signal intensity at this wavelength is relatively insensitive against T_e in the range 1.5-3 eV. Therefore, these distributions can be considered to indicate electron density distributions in the relative scale. It can be seen from Fig. 6 that the LTS signals

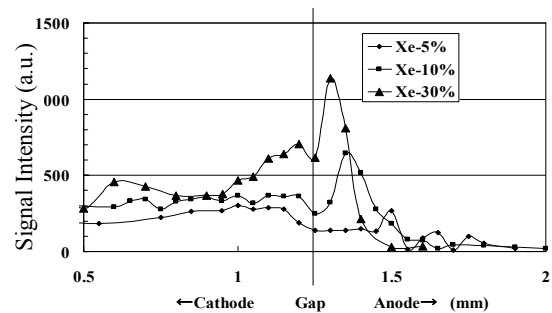


Fig. 6 Distributions of LTS signals along the electrode surface.

increase with the increase of the Xe percentage.

In addition, vertical distributions of n_e above the electrode surface were measured at the gap for different Xe percentages in Fig. 7. Results showed that the positions of the density peaks were found to be inversely proportional to the Xe percentage, being closer to the electrode surface for the higher Xe percentage. This is because the effective mass of the discharge gas becomes heavier for the higher Xe percentage, and then, the diffusion of plasma particles are suppressed for the heavier effective mass of the gas.

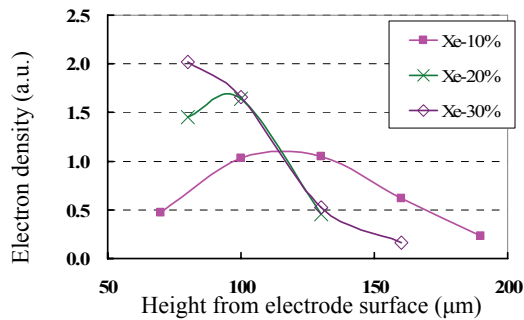


Fig.7 Vertical distribution of n_e above the electrode surface.

3. Preliminary LTS measurements of CCD plasmas

Characteristics of the DBD plasmas which are usually produced between parallel plane electrodes have not yet been understood well. That is because diagnostics of the DBD plasmas are very difficult due to their short life times (< 100 ns) and small sizes (< 100 μm). Moreover, they are produced between plane electrodes randomly both in time and in spatial position. The direct application of the LTS method to usual DBD plasmas is difficult because they can not be controlled spatiotemporally. Therefore, we tried to use a Capacity Coupled Discharge (CCD) instead of the usual DBD. The CCD circuit has a capacitor in series with discharge electrodes. Since the CCD circuit does not have a dielectric layer between discharge electrodes, we can select the shape of the discharge electrodes freely so that we can control the formation time and the spatial position of the CCD plasma. When the discharge conditions are properly selected, characteristics of the CCD plasma can be expected to be similar to those of the DBD plasmas produced between plane parallel electrodes.

An important parameter that assures the similarity between DBD and CCD can be a total electric charge that flows through the discharge channel. In the following experiment, the total charge of CCD was set to be 3×10^{-7} C so that it is not far from that of DBD ($< 3 \times 10^{-8}$ C) and, at the same time, will provide enough number density of electrons for the first attempt of the Thomson scattering measurement.

In the preliminary experiment, the CCD plasmas were generated between a needle electrode and a hemispherical electrode ($\phi=2$ mm). The gap between electrodes was 0.5

mm. The electrical circuit of CCD is shown in Fig. 8. The CCD plasmas were generated in a He gas at a pressure of 400 Torr. The applied voltage was 3 kV and the rise time of the voltage was about 10 ns. The time jitter of the discharge start was around 2 ns, which allowed us to have reproducibility of the LTS signals. The light source of LTS was the second harmonics beam of the Nd:YAG laser. Figure 9 shows an example of LTS spectra observed at the center of the gap and at a time 300 ns after the start of the discharge. From this result, electron density and temperature were evaluated to be $n_e = 7.5 \times 10^{20} \text{ m}^{-3}$, and $T_e = 1.6$ eV.

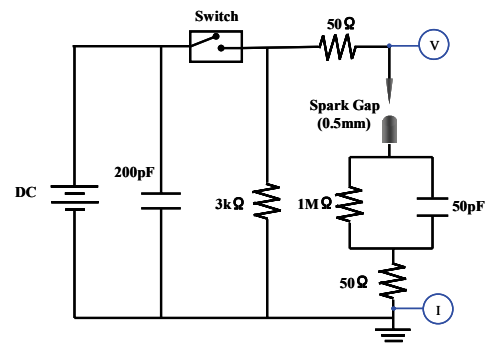


Fig.8 Electrical circuit of CCD.

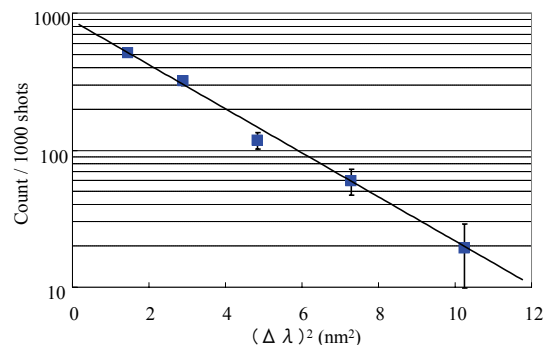


Fig.9 An example of measured LTS spectra from the CCD plasma.

4. Conclusion

We have developed an infrared LTS system. It was found that the system was very effective for measurements of n_e and T_e of PDP micro-discharge plasmas produced in the Ne/Xe gas mixtures. In addition, LTS measurements have been successfully performed on the CCD plasma for the first time.

References

- [1] S. Hassaballa, M. Yakushiji, Y.K. Kim, K. Tomita, K. Uchino, K. Muraoka, IEEE Trans. Plasma Science **32** (2004) 127.
- [2] Y. Yoshioka, A. Okigawa, L. Tessier and K. Toki, IDW' 99, 603.
- [3] S. Hassaballa, Y. Sonoda, K. Tomita, Y.K. Kim and K. Uchino, J. SID **13** (2005) 639.